

Solutions to Problems 3

Chuizheng Kong

November 11, 2024

3

3.1

Consider the motion of a particle around a central object due to a central $1/r^2$ gravity force. We will treat the problem as an IVP, and measure the accuracy of various integration algorithms by comparison to the analytical solution.

3.1.1

Derive the equations of motion for the particle, using a Cartesian coordinate system. Write the equations as a set of coupled 1st-order ODEs. Construct an IC that should give pure circular motion at an orbital radius $r = 1$. Show the analytic expressions of the orbit, and give the value of total energy (kinetic and gravitational) and angular momentum.

Solution: The equation of motion of a particle due to a central $1/r^2$ gravity force (assuming $Gm = 1$ for simplicity) is:

$$\ddot{\mathbf{r}} = -\frac{\mathbf{r}}{r^3} \quad (3.1.1)$$

In Cartesian coordinates, $\mathbf{r} = (x, y)$ and $r = \sqrt{x^2 + y^2}$, so the equations of motion become:

$$\begin{cases} \ddot{x} = -\frac{x}{(x^2 + y^2)^{3/2}} \\ \ddot{y} = -\frac{y}{(x^2 + y^2)^{3/2}} \end{cases} \quad (3.1.2)$$

To convert this 2nd-order system into a set of coupled 1st-order ODEs, we define the velocities: $v_x = \dot{x}$ and $v_y = \dot{y}$. Therefore, the system becomes:

$$\begin{cases} \frac{dx}{dt} = v_x \\ \frac{dy}{dt} = v_y \\ \frac{dv_x}{dt} = -\frac{x}{(x^2 + y^2)^{3/2}} \\ \frac{dv_y}{dt} = -\frac{y}{(x^2 + y^2)^{3/2}} \end{cases} \quad (3.1.3)$$

For a circular orbit of radius $r = 1$, the centripetal acceleration must equal the gravitational acceleration:

$$\frac{v^2}{r} = \frac{1}{r^2} \implies v^2 = \frac{1}{r} = 1 \quad (3.1.4)$$

Therefore, the required speed is $v = 1$. Choosing the initial position and velocity as:

$$\begin{cases} x(0) = 1 \\ y(0) = 0 \\ v_x(0) = 0 \\ v_y(0) = 1 \end{cases} \quad (3.1.5)$$

The particle should execute pure circular motion. The analytical solution for circular motion with angular speed $\omega = v/r = 1$ is:

$$\begin{cases} x(t) = \cos t \\ y(t) = \sin t \end{cases} \quad (3.1.6)$$

The kinetic energy T , gravitational potential energy V , total energy E and angular momentum L are:

$$T = \frac{1}{2}v^2 = \frac{1}{2} \times 1^2 = \frac{1}{2} \quad (3.1.7)$$

$$V = -\frac{1}{r} = -\frac{1}{1} = -1 \quad (3.1.8)$$

$$E = T + V = \frac{1}{2} - 1 = -\frac{1}{2} \quad (3.1.9)$$

$$L = |\mathbf{r} \times \mathbf{v}| = |xv_y - yv_x| = |1 \times 1 - 0 \times 0| = 1 \quad (3.1.10)$$

3.1.2

Write your own forward Euler method from the IC that you just derived.

- Show the particle trajectory for 2 orbital periods using a timestep $\Delta t = 0.01$, and compare with the analytical trajectory.
- Show the position error $|\mathbf{r}_{\text{numeric}} - \mathbf{r}_{\text{analy}}|$ at the end of the integration, for integration timestep of $\Delta t = (0.5, 1, 2, 4) \times 10^{-3}$. Discuss the order of accuracy of the numerical solution based on your results.
- Repeat the above, but for the error in total energy and angular momentum.

Solution: The forward Euler method approximates the solution to the ODEs Equation 3.1.3 using:

$$\begin{cases} x(t + \Delta t) = x + v_x \Delta t \\ y(t + \Delta t) = y + v_y \Delta t \\ v_x(t + \Delta t) = v_x + a_x \Delta t = v_x - \frac{x}{(x^2 + y^2)^{3/2}} \Delta t \\ v_y(t + \Delta t) = v_y + a_y \Delta t = v_y - \frac{y}{(x^2 + y^2)^{3/2}} \Delta t \end{cases} \quad (3.1.11)$$

Using a timestep $\Delta t = 0.01$ and integrating over 2 orbital periods ($t_f = 4\pi$), we obtain both the numerical and analytical trajectories, as illustrated in Figure 1. The plot shows divergence between the numerical and analytical trajectories due to the accumulation of errors in the forward Euler method.

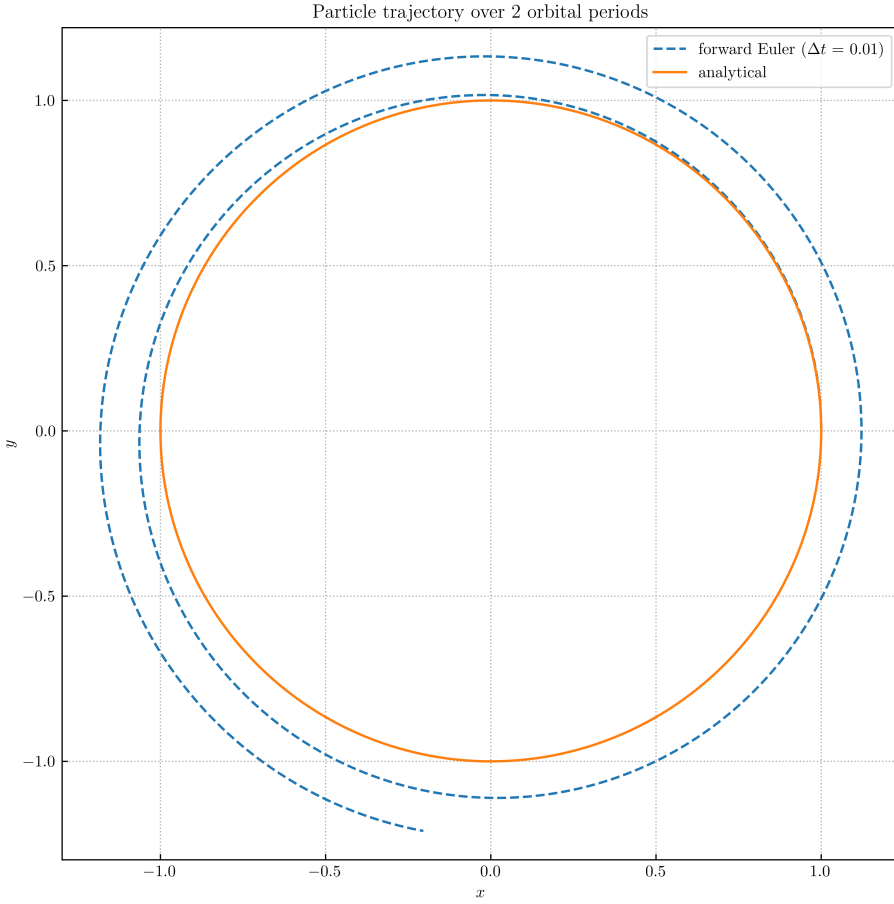


Figure 1: Particle trajectory over 2 orbital periods.

Then we calculate the position, total energy and angular momentum errors at the end of the integration for different timesteps. From the log-log plot Figure 2, we observe that the position error decreases proportionally to Δt . This confirms that the forward Euler method is a 1st-order method, as the error $\delta_f(r)$ scales with the timestep as $\delta_f(r) \propto \Delta t$. The total energy and angular momentum errors also decrease with smaller Δt , but they do not scale linearly due to accumulation over time. The forward Euler method does not conserve energy or angular momentum, leading to unphysical results over long simulations.

3.1.3

Repeat 3.1.2, but using the classic 4th-order Runge-Kutta method. Show the trajectory with $\Delta t = 0.5$, and calculate errors for $\Delta t = 0.05, 0.1, 0.2, 0.4$. What happens when using $\Delta t = 1.0$?

Solution: The RK4 method provides a higher-order accurate solution by considering intermediate slopes

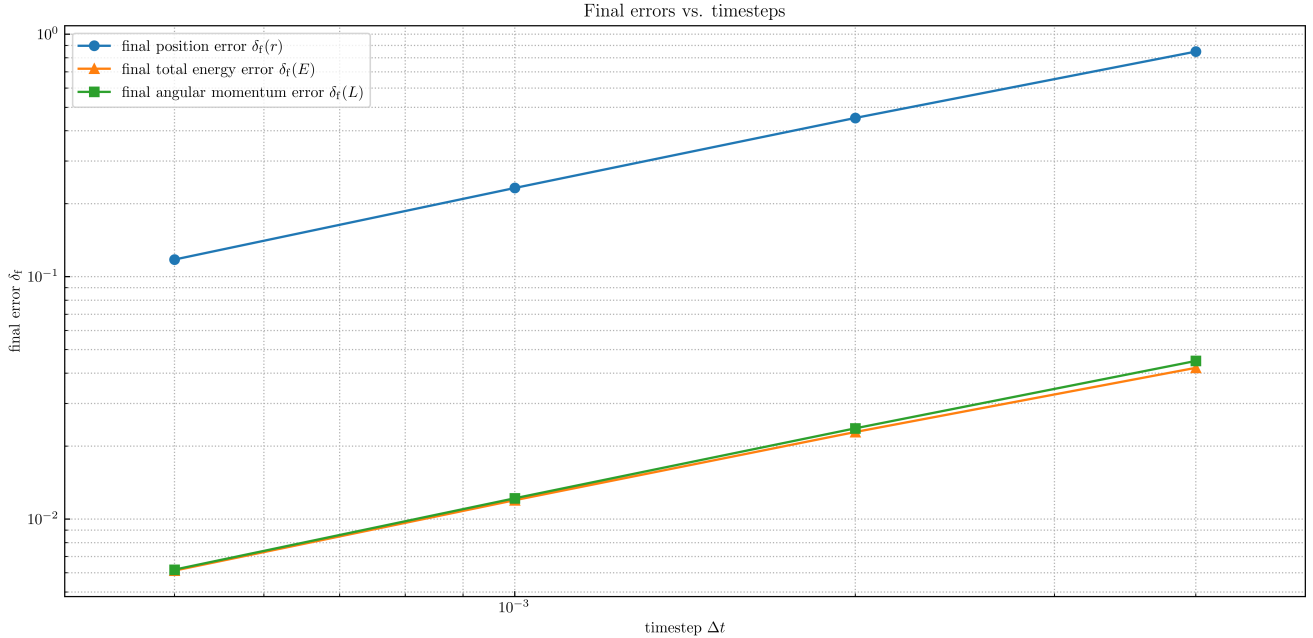


Figure 2: Final errors vs. timesteps.

(increments) within each timestep. For a general 1st-order ODE $dy/dt = f(t, y)$, the RK4 update rule is:

$$\left\{ \begin{array}{l} k_1 = f(t, y) \\ k_2 = f\left(t + \frac{1}{2}\Delta t, y + \frac{1}{2}k_1\Delta t\right) \\ k_3 = f\left(t + \frac{1}{2}\Delta t, y + \frac{1}{2}k_2\Delta t\right) \\ k_4 = f(t + \Delta t, y + k_3\Delta t) \\ y(t + \Delta t) = y + \frac{1}{6}(k_1 + 2k_2 + 2k_3 + k_4)\Delta t \end{array} \right. \quad (3.1.12)$$

We will apply this method to our system of ODEs. We can write Equation 3.1.5 in vector form as:

$$\frac{d\mathbf{y}}{dt} = \mathbf{f}(t, \mathbf{y}) \quad (3.1.13)$$

where $\mathbf{y} = [x, y, v_x, v_y]^T$ and \mathbf{f} is the vector of right-hand sides. Using a relatively large time step $\Delta t = 0.5$, we can integrate the equations over 2 orbital periods ($t_f = 4\pi$), as shown in Figure 3. Despite the large time step, the RK4 method provides a reasonable approximation to the analytical circular orbit. The trajectory remains close to the true circle, demonstrating the superior accuracy of the RK4 method compared to the forward Euler method.

We also compute the position error at the end of the integration for different timesteps $\Delta t = 0.05, 0.1, 0.2, 0.4$. The RK4 method is a 4th-order method, so we expect the position error to scale as $E \propto \Delta t^4$. The plot Figure 4 confirms this behaviour, with errors decreasing rapidly as Δt decreases.

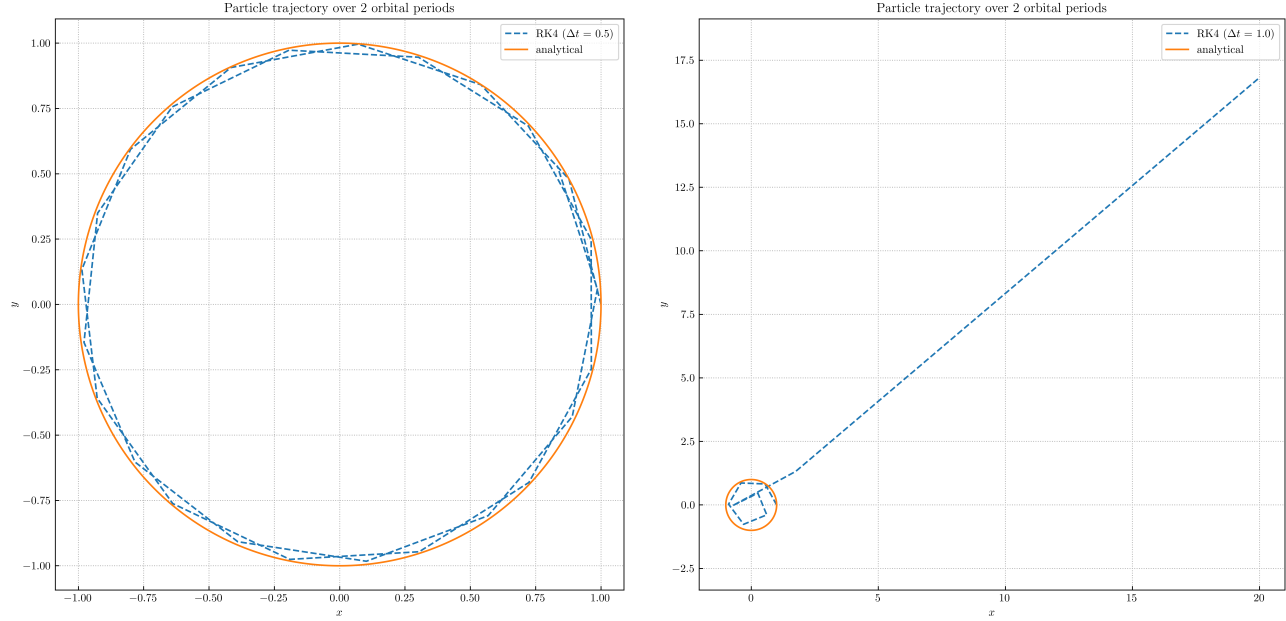


Figure 3: Comparison of particle trajectories over 2 orbital periods.

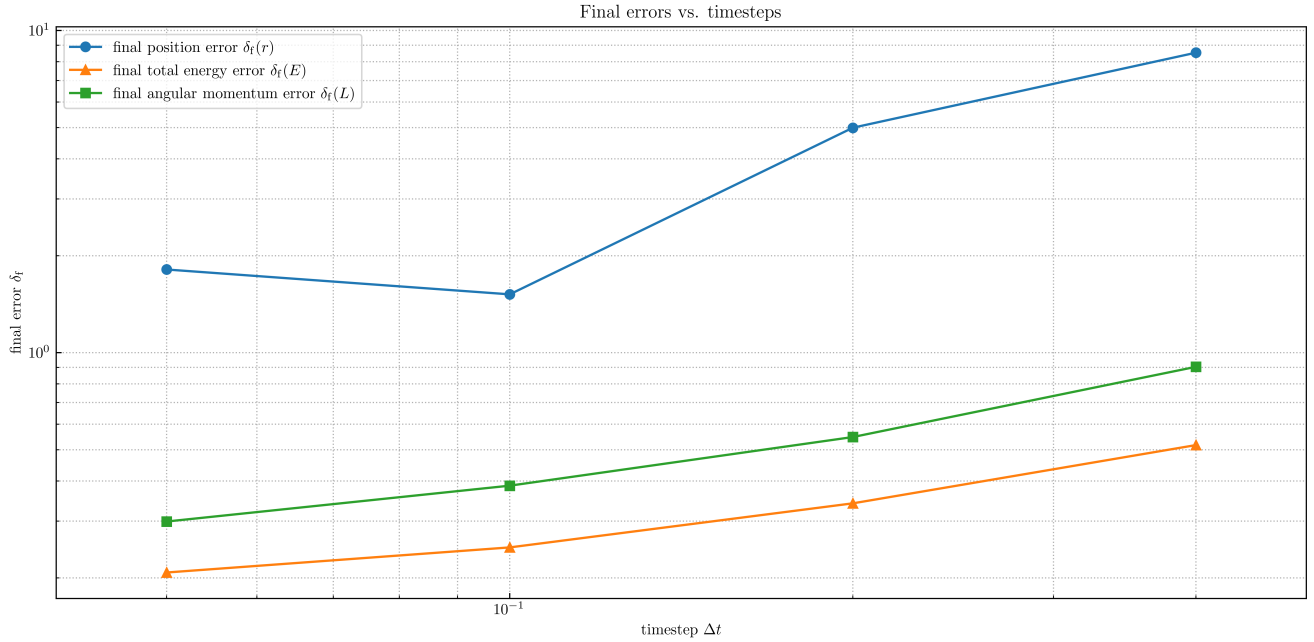


Figure 4: Final errors vs. timesteps.

With $\Delta t = 1.0$, the numerical solution deviates significantly from the analytical trajectory (see in Figure 4). The RK4 method cannot capture the orbital dynamics with such a large timestep. This demonstrates that even higher-order methods have limitations when the timestep is too large relative to the timescale of the system.

3.1.4

Write your own leapfrog integrator and integrate the same equations as in 3.1.2 and 3.1.3 but for 10 orbits. Show the particle trajectory with $\Delta t = 0.3$, as well as the *time evolution* of the position error, and error in energy and angular momentum. To what extent does the method conserve total energy and angular momentum? Where is the source of position error?

Solution: The leapfrog method updates positions and velocities in a staggered manner:

$$\left\{ \begin{array}{l} v_x(t + \frac{1}{2}\Delta t) = v_x - \frac{1}{2} \frac{x}{(x^2 + y^2)^{3/2}} \Delta t \\ v_y(t + \frac{1}{2}\Delta t) = v_y - \frac{1}{2} \frac{y}{(x^2 + y^2)^{3/2}} \Delta t \\ x(t + \Delta t) = x + v_x(t + \frac{1}{2}\Delta t)\Delta t = X \\ x(t + \Delta t) = x + v_x(t + \frac{1}{2}\Delta t)\Delta t = Y \\ v_x(t + \Delta t) = v_x - \frac{1}{2} \frac{X}{(X^2 + Y^2)^{3/2}} \Delta t \\ v_y(t + \Delta t) = v_y - \frac{1}{2} \frac{Y}{(X^2 + Y^2)^{3/2}} \Delta t \end{array} \right. \quad (3.1.13)$$

We integrate the equations over 10 orbital periods ($t_f = 20\pi$) with a timestep of $\Delta t = 0.3$ (see in Figure 5).

Next, we analyze the time evolution of the position error, and the errors in total energy and angular momentum (see in Figure 6). The leapfrog integrator shows excellent conservation of total energy over long timescales. The energy error remains bounded and does not grow significantly over time. Similarly, the leapfrog method conserves angular momentum very well. The errors in angular momentum are small and do not accumulate over time, indicating that the method preserves this conserved quantity. Despite the good conservation properties, the position error grows over time. This is due to the phase error inherent in numerical integration methods. The leapfrog method conserves energy and angular momentum but may introduce small phase shifts in the motion, causing the numerical trajectory to lag or lead the analytical solution over many orbits.

3.2

3.2.1

The interstellar medium consists of gas and dust, who interact by mutual aerodynamic drag. For a dust of given size, the drag law is expressed as

$$\frac{dv_d}{dt} = -\frac{v_d - v_g(t)}{t_s} \quad (3.2.1)$$

where v_d , $v_g(t)$ are the velocities of gas and dust, and t_s is the stopping time, determined by dust size and gas density. For simplicity, we only consider a 1D problem here and t_s is constant. We need to write an

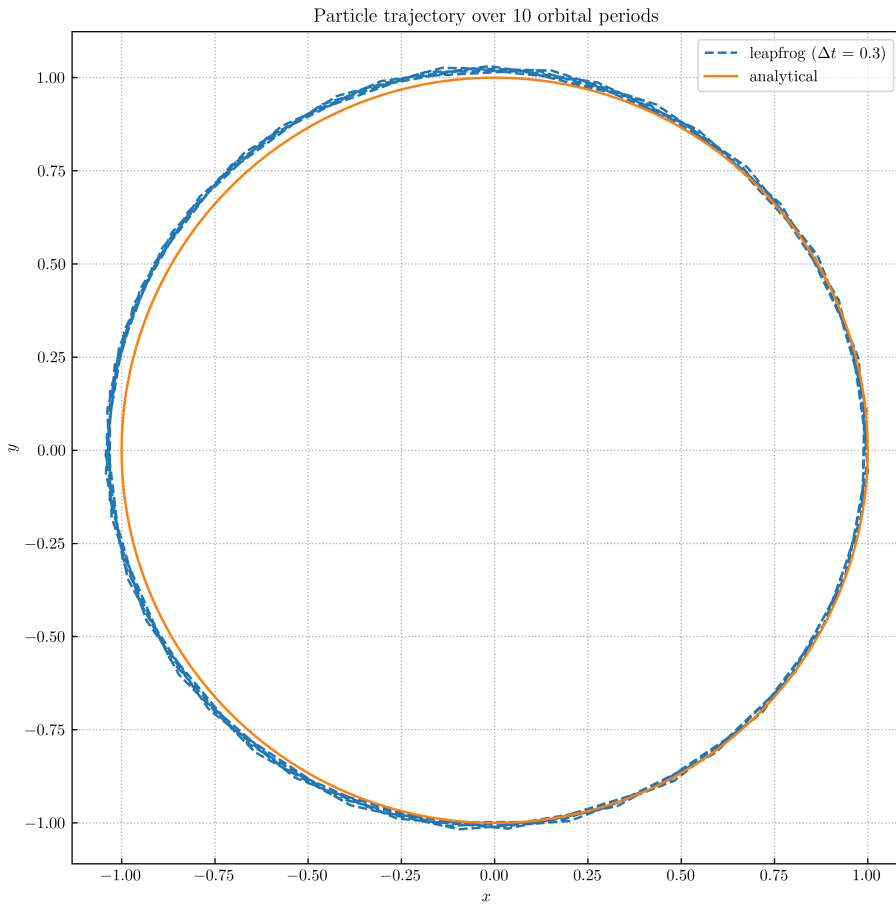


Figure 5: Particle trajectory over 2 orbital periods.

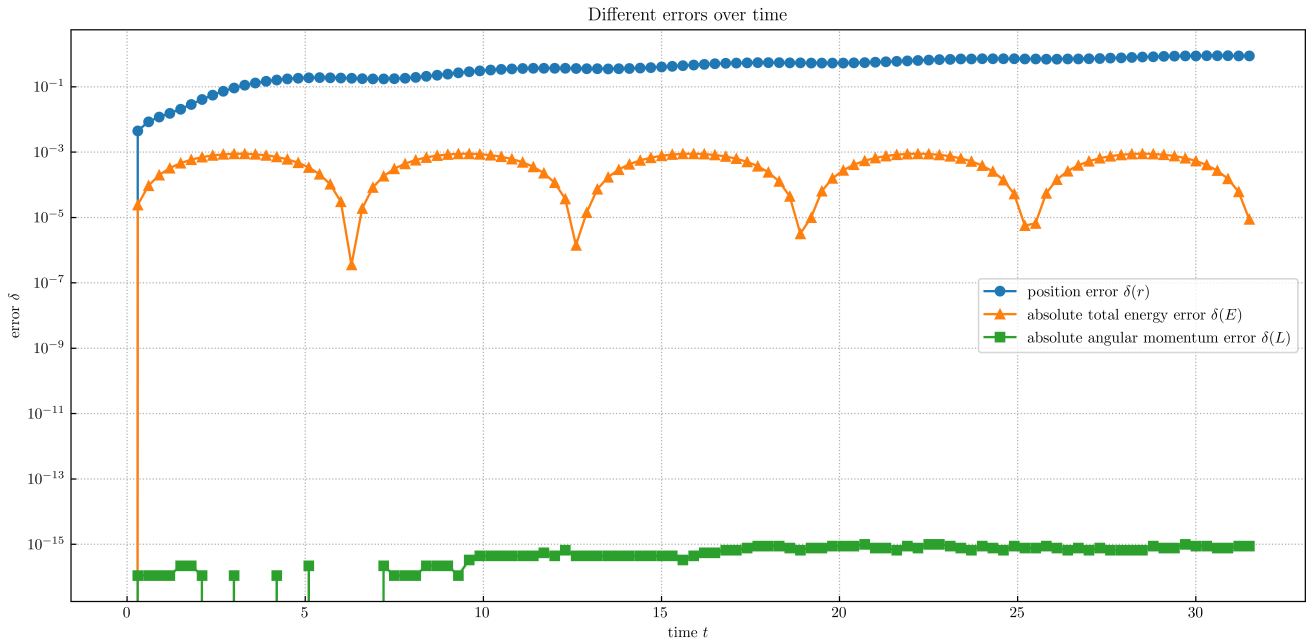


Figure 6: Different errors over time.

ODE solver to integrate Equation 3.2.1 from time 0 to T . Discuss under what circumstances the equation can become stiff, and what would be the general strategy to design your integrator (you can mention what method to use, but no need to provide detailed algorithm here).

Solution: We can rewrite the 1st-order linear ODE as:

$$\frac{dv_d}{dt} + \frac{1}{t_s} v_d = \frac{v_g(t)}{t_s} \quad (3.2.2)$$

The equation becomes stiff when the stopping time t_s is much smaller than the characteristic timescale over which $v_g(t)$ varies or the total simulation time T : $t_s \ll T$. In this regime, the term $\frac{v_d}{t_s}$ becomes dominant, leading to rapid changes in v_d . Consequently, explicit integration methods require very small time steps Δt (with $\Delta t \ll t_s$) to maintain numerical stability, making the integration computationally intensive. To handle both stiff and non-stiff regimes efficiently, the following strategies can be employed: backward Euler, Trapezoid/Crank-Nicholson, implicit Runge-Kutta(e.g. Kaps-Rentrop) and implicit multi-step (e.g. backward differentiation formula, BDF) methods.

3.2.2

In reality, interstellar dust is characterized by a size distribution, and hence dust of different sizes have different t_s . Moreover, due to momentum conservation, gas should feel the back reaction from dust, whose dynamics is also affected by dust motion. If we discretize the dust size distribution into M bins, with the i -th ($i = 1, \dots, M$) bin characterized by a dust species with stopping time $t_{s,i}$, and a dust-to-gas mass ratio ε_i , the composite equations of motion in a uniform medium read

$$\begin{cases} \frac{dv_{d,i}}{dt} = -\frac{v_{d,i} - v_g(t)}{t_{s,i}} \\ \frac{dv_g}{dt} = \sum_{i=1}^M \varepsilon_i \frac{v_{d,i} - v_g}{t_{s,i}} \end{cases} \quad (3.2.3)$$

where now $v_{d,i}$ represents the velocity of each dust species. For our purpose, t_i and ε_i are considered to be constants. Generalize your discussions in 3.2.1 to handle Equation 3.2.3 on when the equations become stiff, and how you would design your integrator.

Solution: The stiffness of the system increases due to wide range of stopping times and back reaction coupling. If the dust species have stopping times $t_{s,i}$ that vary across several orders of magnitude, the fastest dynamics (small $t_{s,i}$) impose severe restrictions on the timestep Δt . The inclusion of back reaction couples the dust and gas velocities, meaning that rapid changes in dust velocities influence the gas velocity and vice versa. Stiffness arises when at least one $t_{s,i}$ is much smaller than the total simulation time T : $\min(t_{s,i}) \ll T$. To integrate Equation 3.2.3 efficiently across all regimes, we can also use implicit integration methods (e.g. backward Euler, Trapezoid/Crank-Nicholson, Kaps-Rentrop and BDF) that are stable for stiff systems.

3.2.3

Suppose that accuracy is NOT our primary concern. Give your integration algorithm so that you can integrate both Equation 3.2.1 and Equation 3.2.3 in all regimes (non-stiff and stiff) as an IVP. Comment on whether your algorithm conserves total momentum at the level of machine precision.

Solution: We use the implicit Euler method. At each step n with timestep Δt for Equation 3.2.1:

$$v_d^{(n+1)} = v_d^{(n)} - \frac{v_d^{(n+1)} - v_g(t)}{t_s} \Delta t \quad (3.2.4)$$

Rearranged to:

$$v_d^{(n+1)} = \frac{v_d^{(n)} t_s + v_g(t) \Delta t}{t_s + \Delta t} \quad (3.2.5)$$

For Equation 3.2.3:

$$\begin{cases} v_{d,i}^{(n+1)} = v_{d,i}^{(n)} - \frac{v_{d,i}^{(n+1)} - v_g^{(n+1)}}{t_{s,i}} \Delta t \\ v_g^{(n+1)} = v_g^{(n)} + \sum_{i=1}^M \varepsilon_i \frac{v_{d,i}^{(n+1)} - v_g^{(n+1)}}{t_{s,i}} \Delta t \end{cases} \quad (3.2.6)$$

Rearranged to:

$$\begin{cases} \left(1 + \frac{\Delta t}{t_{s,i}}\right) v_{d,i}^{(n+1)} - \frac{\Delta t}{t_{s,i}} v_g^{(n+1)} = v_{d,i}^{(n)} \\ - \sum_{i=1}^M \varepsilon_i \frac{\Delta t}{t_{s,i}} v_{d,i}^{(n+1)} + \left(1 + \sum_{i=1}^M \varepsilon_i \frac{\Delta t}{t_{s,i}}\right) v_g^{(n+1)} = v_g^{(n)} \end{cases} \quad (3.2.7)$$

Then use a linear solver (e.g., LU decomposition, direct solver) to solve for $v_{d,i}^{(n+1)}$ and $v_g^{(n+1)}$. The total momentum p is:

$$p = v_g + \sum_{i=1}^M \varepsilon_i v_{d,i} \quad (3.2.8)$$

While the implicit Euler method is stable and suitable for stiff equations, it does not inherently conserve the total momentum at the level of machine precision due to numerical errors from discretization and round-off.

3.2.4

Using your integrator for Equation 3.2.1, solve the IVPs with $v_d(0) = 0$ and integrate the equation to $T = 10$ for the following 3 cases:

1. $v_g = t_s = 1$. Show the time evolution of v_d from your numerical solution. Compare with analytical solution and discuss the accuracy of your algorithm.
2. $v_g = \sin t$, $t_s = 1$. Show the time evolution of v_d from your numerical solution.
3. $v_g = \sin t$, $t_s = 10^{-5}$. Show the time evolution of v_d from your numerical solution.

Solution:

1. Since $v_g = t_s = 1$, the analytical solution is:

$$\frac{dv_d}{dt} = -\frac{v_d - v_g(t)}{t_s} = 1 - v_d \implies v_d = 1 - e^{-t} \quad (3.2.9)$$

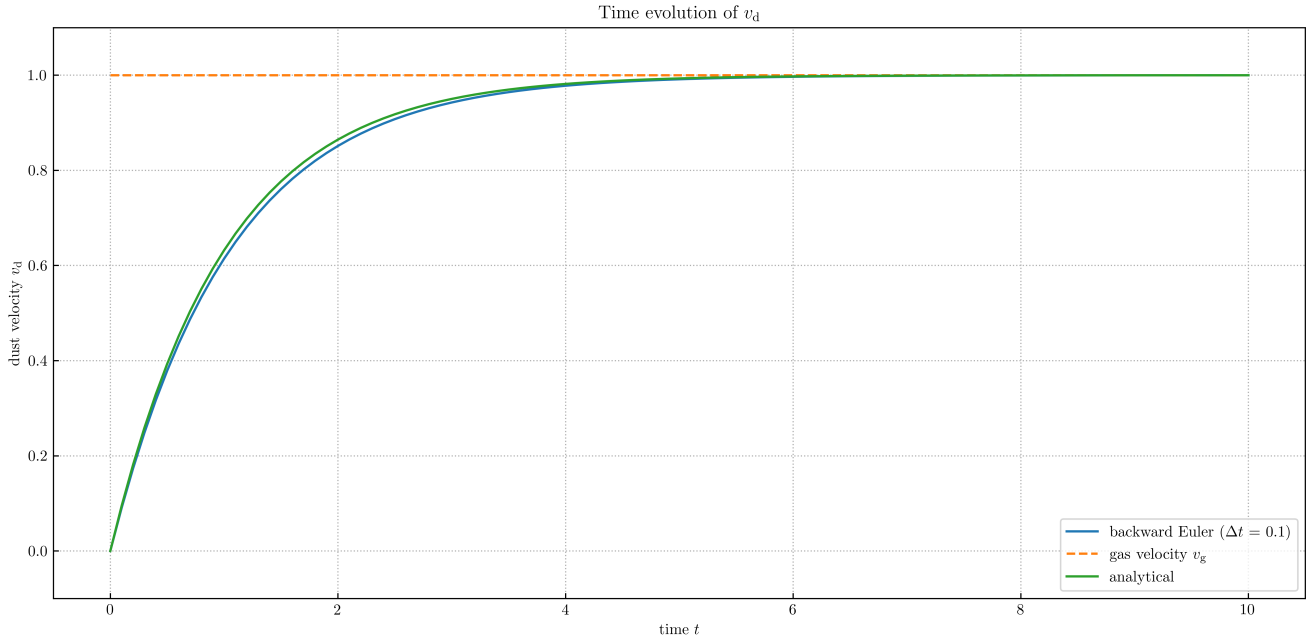


Figure 7: Time evolution of v_d

The numerical solution closely follows the analytical solution, demonstrating the accuracy of the backward Euler method for this case. The slight discrepancies are due to the timestep; reducing Δt would improve the accuracy.

2. When $v_g = \sin t$ and $t_s = 1$, the time evolution of v_d is shown in Figure 8. The dust velocity v_d follows the gas velocity v_g with some lag due to the stopping time. The backward Euler method captures this behaviour accurately.

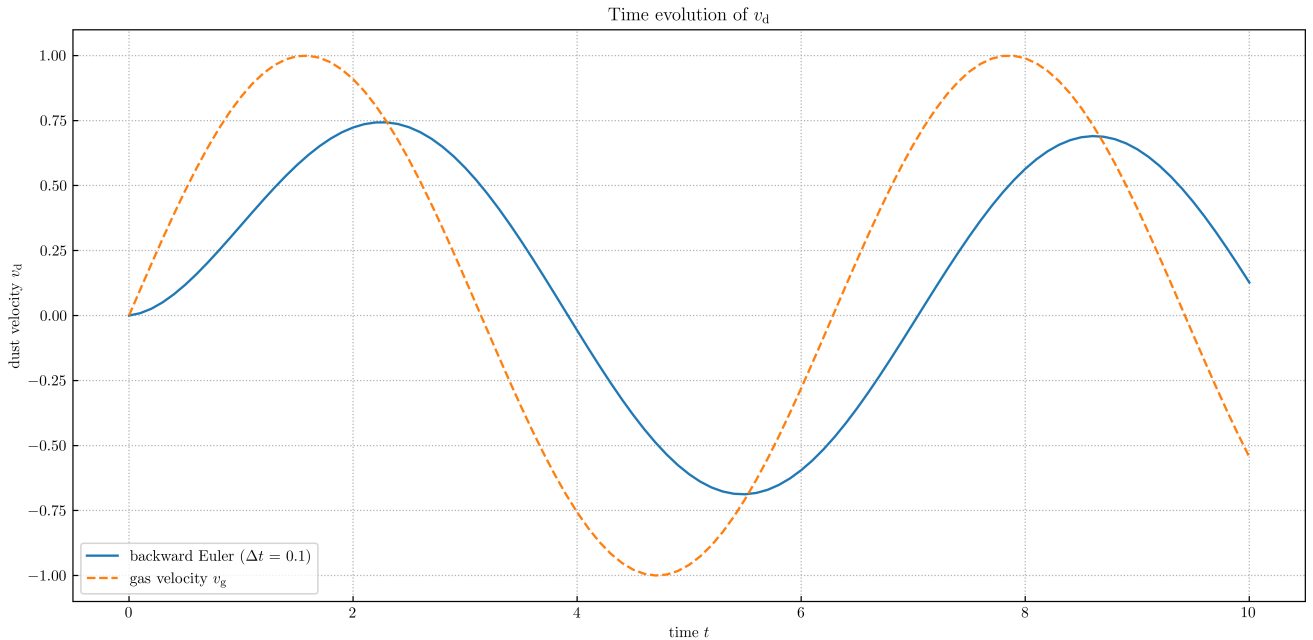


Figure 8: Time evolution of v_d .

3. When $v_g = \sin t$ and $t_s = 10^{-5}$, the time evolution of v_d is shown in Figure 9. A very small stopping time represents a stiff problem. Because t_s is very small, the dust velocity rapidly aligns with the gas velocity, and $v_d \approx v_g$. The backward Euler method handles this stiff problem without requiring a reduced timestep, showcasing its stability.

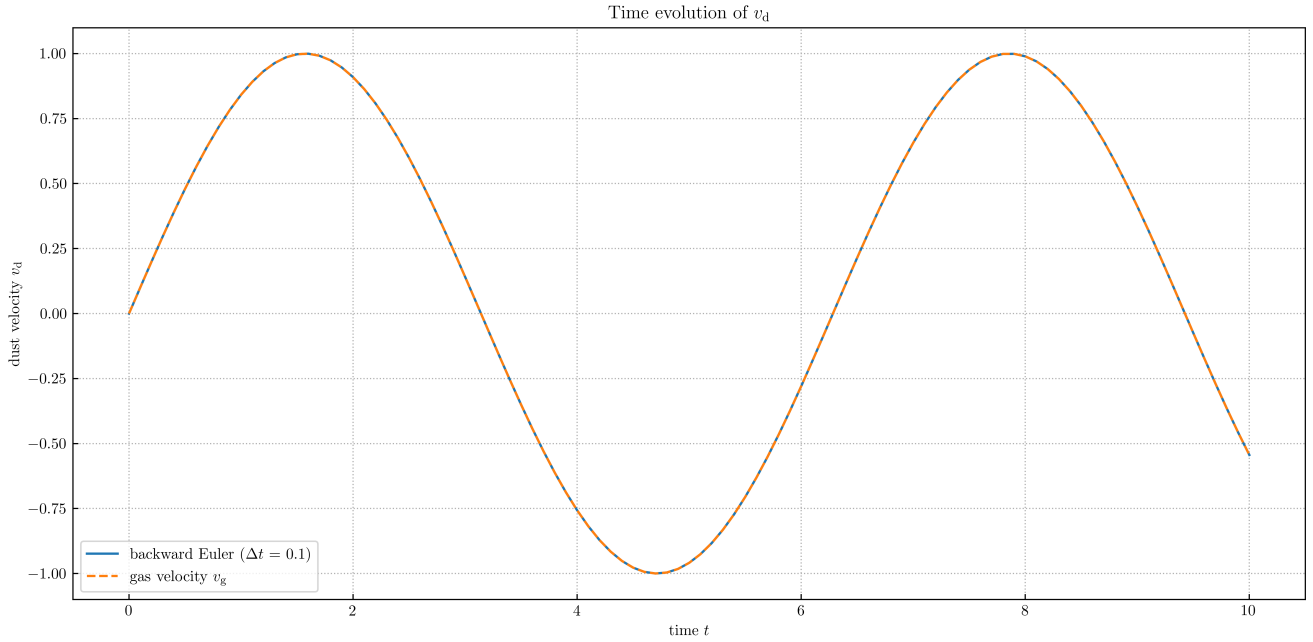


Figure 9: Time evolution of v_d .

3.2.5

Consider 10 dust species, with stopping time being $t_{s,i} = 10^{-6+i}$ ($i = 1, 2, \dots, 10$) and $\varepsilon_i = 0.1$ for each species. For IC, let $v_{d,i} = 0$ and $v_g = 1$. Solve Equation 3.2.3 to time $T = 10^5$. To show your solution, make the following 2 plots:

1. Show the time evolution of gas velocity and the velocities of the first 5 dust species, for the first 10 steps.
2. Show the time evolution of gas velocity and the velocities of the remaining 5 dust species, with time shown as $\lg t$.

Solution:

1. In the 1st 10 steps (see in Figure 10), the gas velocity remains close to the initial value since the dust species have not had sufficient time to influence it significantly. The dust species with smaller stopping times (species 1-5) begin to accelerate due to the gas drag force.
2. On a logarithmic time scale (see in Figure 11), we can see that the velocities of the remaining dust species (species 6-10) evolve over a longer time due to their larger stopping times. Eventually, all dust species velocities approach the gas velocity, and the system reaches a steady state.

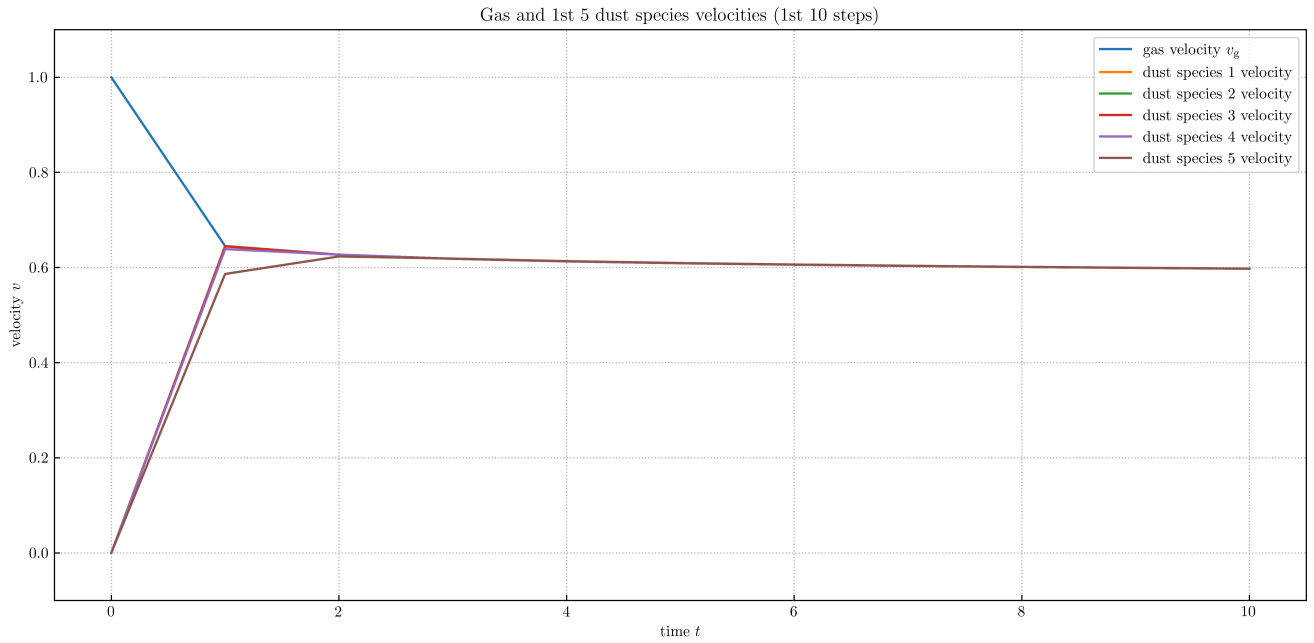


Figure 10: Gas and 1st 5 dust species velocities (1st 10 steps).

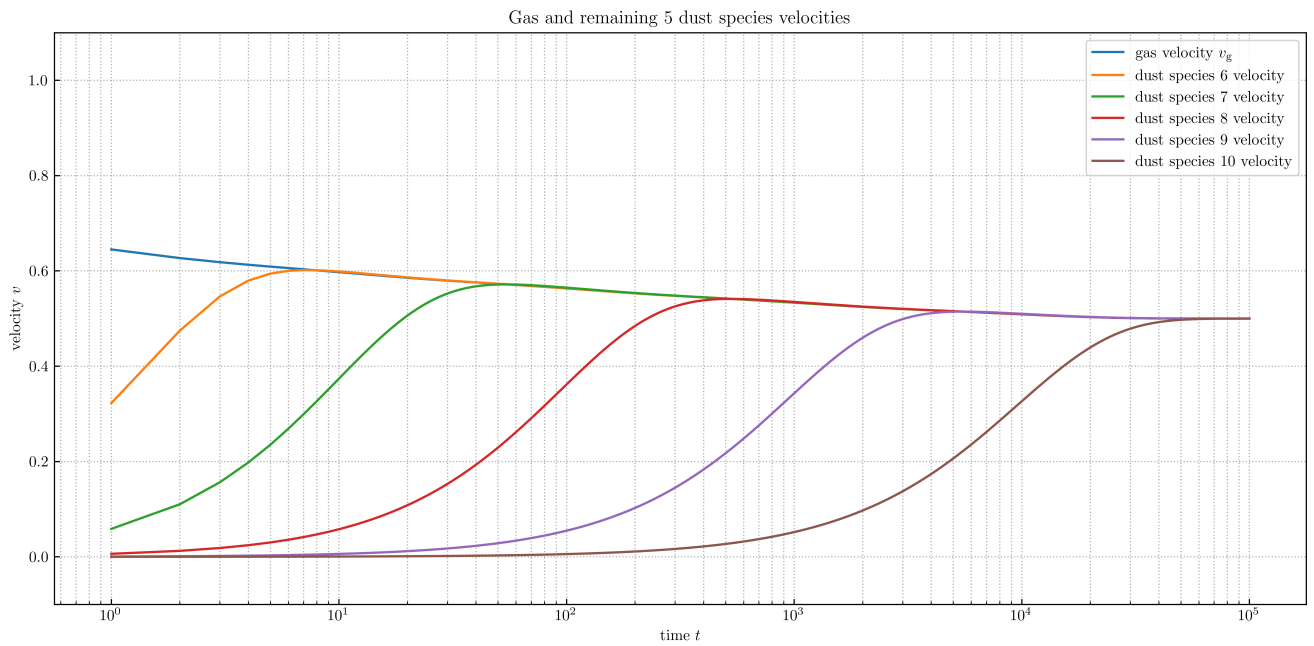


Figure 11: Gas and emaining 5 dust species velocities.